Adaptive Snapshot Routing Based on Space Debris Risk Perception in Satellite Optical Networks

Zhuangzhuang Ma
State Key Laboratory of Information Photonics and Optical Communications
Beijing University of Posts and Telecommunications
Beijing, China
mzz@bupt.edu.cn

Yongli Zhao
State Key Laboratory of Information Photonics and Optical Communications
Beijing University of Posts and Telecommunications
Beijing, China
yonglizhao@bupt.edu.cn

Wei Wang
State Key Laboratory of Information Photonics and Optical Communications
Beijing University of Posts and Telecommunications
Beijing, China
weiw@bupt.edu.cn

Xiangjun Xin
State Key Laboratory of Information Photonics and Optical Communications
Beijing University of Posts and Telecommunications
Beijing, China
xjxin@bupt.edu.cn

Jie Zhang
State Key Laboratory of Information Photonics and Optical Communications
Beijing University of Posts and Telecommunications
Being, China
Jie.zhang@bupt.edu.cn

***Abstract*—With the advantages of large transmission capacity, high data rate and good confidentiality, inter-satellite laser communication has become a promising alternative for satellite networks. However, with more and more satellite nodes being launched into the space, the number of space debris will increase rapidly. Due to the nature of linear transmission of laser links, space debris may cause the uncertain interruption of laser links, and further degrade the link survivability of satellite optical networks. In this paper, we design a risk perception model based on machine learning for inter-satellite laser links risk caused by space debris. Based on this model, we propose an adaptive snapshot routing strategy based on flexible granularity (ASRS-FG), which can effectively avoid the risk of inter satellite link interruption caused by space debris. Finally, to verify the performance of the algorithm, we built a satellite optical networks simulation platform. The simulation results show that our model's prediction accuracy on space debris risk reaches 95%. Compared with the equal-length snapshot routing strategy (ESRS), ASRS-FG effectively avoids the use of risky laser links and achieves higher service success ratio and fewer snapshot switching times.**

Keywords—Satellite optical networks, space debris, risk perception, machine learning, adaptive snapshot routing

I. INTRODUCTION

Space debris refers to the products of human space activities, including rocket bodies and satellite bodies that complete missions, rocket ejections, etc., and they are the main pollution sources of space environment. Since the launch of the first artificial satellite in 1957, more and more space activities have led to a rapid increasing in the number of spacecrafts in orbit A series of space collision accidents and anti-satellite tests have produced more and more space debris and thus caused more severe pollution to the space environment [1]. According to the statistics from North American Air Defense Command (NORAD), as of the beginning of 2020, there have been nearly 30,000 space debris larger than 10 cm in diameter, and more than 900,000 dangerous space debris between 1 cm and 10 cm, with a total mass of more than 8,000 tons. Meanwhile, compared with microwave communication, laser communication has the advantages of high transmission rate, large transmission capacity, high speed, good confidentiality and low power consumption of terminal equipment , and thus it has become the inevitable option of future satellite networks [2-3]. In order to cover the global earth, satellite optical networks will consist of tens of thousands of satellites in low earth orbit in the future, such as the Starlink project. The satellite nodes communicate with each other through point-to-point or point-to-multipoint laser links [4] to achieve large-capacity transmission. Since a large amount of space debris is mainly concentrated in low earth orbit [5], there must be some debris moving over the linear links between two satellites, forming a three-point collinear phenomenon. Such case will lead to the interruption of the inter satellite link, and then reduce the quality of satellite communication service, as shown in Fig. 1.

In addition, due to the existence of orbital descent and secondary collision named Kessler syndrome [6-7] of space debris, the trajectory of the debris is uncertain, and thus the risk of inter-satellite link interruption is uncertain as well in satellite optical networks. Machine learning is widely used in various network use cases [8], because a well-trained model is good at predicting future events. Space debris trajectory prediction and removal based on artificial intelligence has been studied. For example, reference [9] proposes a solution to actively remove multiple debris based on reinforcement learning, and reference [10] proposes a debris orbit prediction strategy based on supervised learning. What's more, a collision prediction method of space debris and LEO satellite based on machine learning is proposed in reference [11]. The existing works on space debris mainly focused on orbital observations, environmental modeling, spacecraft protection, and how to avoid collisions with spacecraft, etc. However, to the best of our knowledge, the

978-3-903176-33-1 © 2021 IFIP

communication interruption problem that is caused by space debris, is not well studied yet.

What's more, in order to save the limited satellite storage space and to reduce signaling overhead caused by topology information exchange, satellite optical networks usually adopt virtual topology routing strategy [12], such as equal-length snapshot routing strategy (ESRS). However, ESRS lacks the flexibility of snapshot division and cannot adjust the length of the snapshot according to the distribution of link risks caused by debris. Meanwhile, the current routing algorithm does not consider the impact of space debris on the link, and cannot effectively avoid the use of risky links.

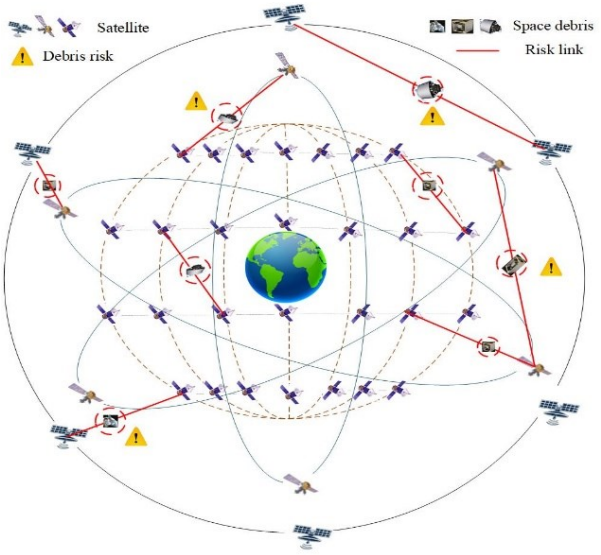

Fig. 1. Laser link risk caused by space debris

II. LINK RISK PREDICTION MODEL CAUSED BY SPACE DEBRIS

In this section, we introduce the physical model of laser link interruption caused by space debris , and analyze the duration of link interruption caused by space debris with different sizes and trajectories. In the following sub-section, we propose a space debris risk perception model, and analyze the performance of this model.

A. Physical Model of Laser Link Interruption Caused by Space Debris

Hundreds of millions of debris are active in space, and are mainly concentrated near low earth orbit. These debris have different trajectories, sizes and speeds, which leads to different inter-satellite laser links interruption time. For example, when debris of the same size and speed intersect the inter-satellite link along different trajectories, the interruption time of the link will show a great difference. In view of the different link interruption scenarios of the low-orbit satellite optical networks, we grasp the main influencing factors such as debris speed, size, trajectory, and intersection method, and construct the corresponding physical model. Taking into account the spatial position relationship, the critical value of the interruption of the inter-satellite laser link caused by the debris is divided into the following three cases: case 1 of the debris trajectory intersects the link vertically, case 2 of generally intersects, and case 3 of special tangent. As shown in Fig. 2, case 1 depicts the physical model of vertical intersection, since the size of the debris is much smaller than the semi-major axis of the debris trajectory, the debris trajectory can be approximated as a line segment during the interruption. Under the premise of the intersection, this situation represents the minimum interruption time caused by debris of the same size to the link. 2. The function of link interruption time caused by different size debris in case 1 is given by the following expression, and the calculation results are as shown in Table I.

$$t = \frac{d+w}{v} \tag{1}$$

Where t is the interruption time caused by debris, d is the size of the debris, the typical value of v is 8 km/s, which represents the debris velocity, and the typical value of w is 10 mm, which represents the laser beam width.

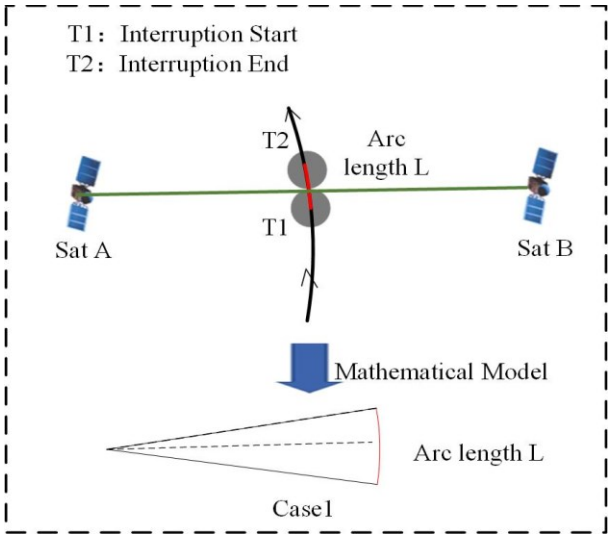

Fig. 2. Physical model of vertical intersection

TABLE I. INTERRUPTION TIME IN CASE 1

Size(mm)	1	10	50	100
Time(ms)	0.0025	0.0138	0.0638	0.1263

As shown in Fig. 3, case 2 describes the general physical model of the intersection between the debris track and the link. When the link distance is long, it is more likely to have two intersections, as shown in Fig. 3 (a). If the link distance is short, it is more likely to have a single intersection, as shown in Fig. 3 (b). The function of link interruption time caused by different size debris in case 2 is given by the following expression, and the calculation results are as shown in Table II.

$$t = \frac{2d}{v\sin\beta} \tag{2}$$

Where t is the interruption time caused by debris, d is the size of the debris, the typical value of v is 8 km/s, which represents the debris velocity, and $0<\beta<90°$.

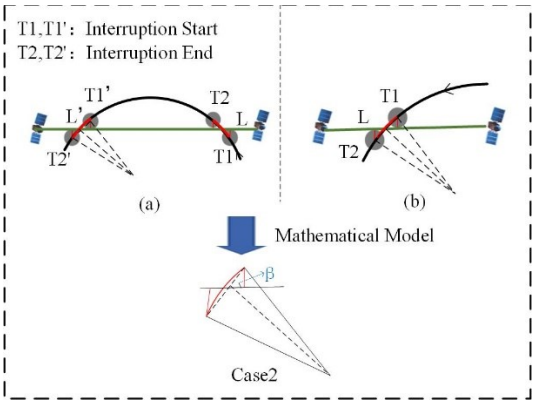

Fig. 3. Physical model of general intersection

TABLE II. INTERRUPTION TIME IN CASE 2

Size/mm	1	10	50	100
Time/ms	0.125/8sinβ	1.25/sinβ	6.25/sinβ	12.5/sinβ

As shown in Fig. 4, case 3 depicts the physical model of the debris trajectory exactly crosses the link and is tangent to it, which represents the maximum interruption time that debris of the same size and speed can reach. The function of link interruption time caused by different size debris in case 3 is given by the following expression, and the calculation results are as shown in Table III.

$$\theta = \cos^{-1}(1 - \frac{d}{a}) \quad (3)$$

$$t = \frac{2\theta L}{360v} \quad (4)$$

Where t is the interruption time caused by debris, d is the size of the debris, the typical value of a is 7158 km, which represents the orbit radius of debris, the typical value of v is 8 km/s, which represents the debris velocity, and 0<θ<90°.

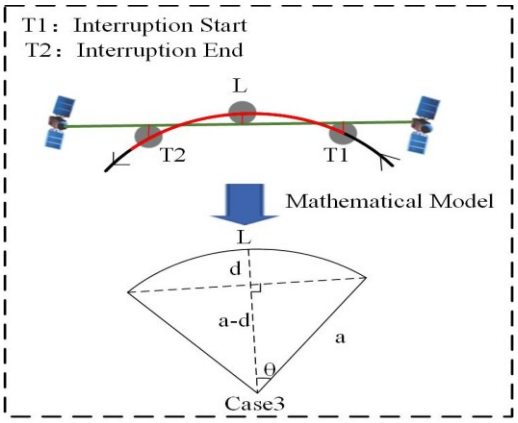

Fig. 4. Physical model of special tangent

TABLE III. INTERRUPTION TIME IN CASE 3

Size(mm)	1	10	50	100
Time(ms)	93.875	296.858	663.796	938.749

According to the above results, the longest inter satellite laser link interruption time caused by debris reaches 938.749 ms, while the transmission delay of single hop low orbit inter satellite laser link is only about 10 ms and he tolerable delay of voice communication is about 150 ms, which also seriously affects the quality of service in satellite optical networks. Links with an interruption time of less than 10 ms are classified as zero-risk links, which of between 10 ms and 150 ms are classified as low-risk links, and which of greater than 150 ms are classified as high-risk links.

B. Space Debris Risk Perception Model

According to the physical model in the previous part, it can be seen that the length of the link interruption time is closely related to the debris trajectory, speed and other factors. The K-Means algorithm is used to cluster 4096 sets of the Two Line Elements (TLE) of space debris from NORAD. These data include the debris orbital inclination, the ascension of the ascending node, the number of circles per day, the position versus time, etc. Machine learning has high accuracy in predicting future events and classification. We take a number of different K values, and find that the data set obtained when k = 3 is consistent with analysis results of link interruption time in the above sub-section. Then we label the three types of data sets obtained by clustering as zero-risk, low-risk and high-risk respectively. We train the classification model by using these three data sets, and filter the zero-risk data set. We can get the orbit data of debris of low and high-risk debris sets from relevant testing institutions ,such as Space Debris Monitoring and Application Center. Then we use the low and high-risk debris orbit data and satellite orbit data as the input, and use three-point collinear relationship in space and expression (1) - (4) as the judgment basis to get the risky link ID and link interruption start and end time. When training the debris data classification model, the ReLU excitation function, Cross-Entropy loss function, and stochastic gradient descent (SGD) optimizer are used, and the hidden layer contains 10 nerves. The accuracy curve and training time for debris risk classification are shown in Fig. 5. Since only 4096 sets of data are trained, the training time is basically about 10s. It can be seen that as the learning rate increases, the accuracy first increases and then decreases, when the learning rate is 0.02, the prediction accuracy rate is up to 95%. And when the learning rate is over 0.02, as the learning rate increases, the training time decreases, but the accuracy rate also decreases, because when the learning rate is large, the step of gradient descent is too large, it may cross the optimal value, and the model has an underfitting problem.

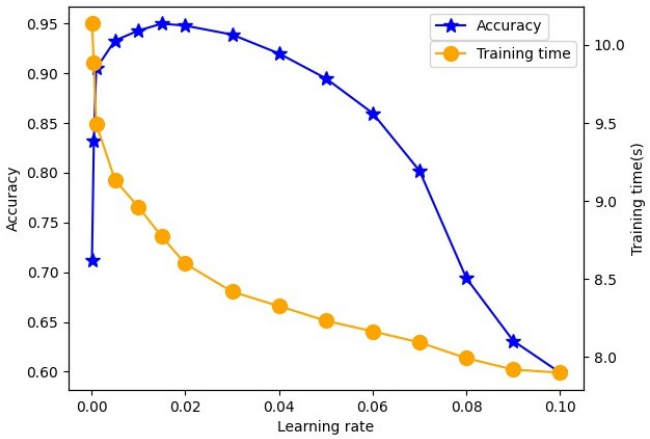

Fig. 5. Debris classification accuracy and training time

III. ADAPTIVE SNAPSHOT ROUTING STRATEGY BASED ON FLEXIBLE GRANULARITY

In the previous section, the space debris risk perception model outputs the ID of the link affected by the debris and the start and end time of the link interruption. Avoiding the use of risky links can improve the service transmission success rate. Meanwhile, Reducing the number of snapshot switching can also improve the service success rate. In order to make full use of inter satellite link resources and improve routing and transmission performance, we propose an adaptive snapshot routing strategy based on flexible granularity (ASRS-FG). As shown in Fig. 6, because the dynamic changes of satellite optical networks topology are predictable , we divide the network topology in a constellation period into multiple minimum snapshot granularity (MSG), all MSGs are equal in length and are the basic unit of snapshot. We allocate the MSGs affected by space debris into a single snapshot, which can solve the problem that a high-risk link for only a few seconds cannot be used within a few minutes of snapshots. This problem reduces the utilization rate of inter-satellite links, and also affects the routing and transmission performance. However, when it solves the problem of snapshot flexibility and the availability time ratio of link resources, due to the short snapshot granularity and the short interval of high-risk link occurrence time, the topology snapshot length is too short. In other words, the number of snapshots is too large, the snapshot switching is too frequent, the stability of satellite optical networks is poor, and it takes up too much satellite storage space.

In order to resolve the contradiction between the number of snapshots and the average link available time, occupy less on-board storage space, and improve service success ratio, the division of snapshot intervals needs to meet certain constraints. Specifically, we use L minutes as the MSG, and all the snapshot lengths are integer multiples of this granularity, that is n*L, where n is a positive integer. For multiple adjacent granularities without link risk caused by debris, the snapshot length is T minutes [13-14], that is, the snapshot contains T/L MSGs. If the MSGs containing link risks are adjacent, they are divided into the same snapshot. In addition, the link risk interval does not span two snapshots, that is, if a certain link risk interval happens to be at the demarcation point of the basic granularity, the two MSGs belong to the same snapshot. As shown in Fig. 6, the adjacent black line interval is a MSG, and multiple MSGs in a bracket forms a snapshot. The green range represents the time period without debris risk, and the red range represents the period with debris risk. Fig. 6 shows that T takes 5 minutes and L takes 1, 1.25, and 2.5 minutes respectively. This strategy only pays a small amount of link average available time to achieve a significant reduction in snapshot switching times.

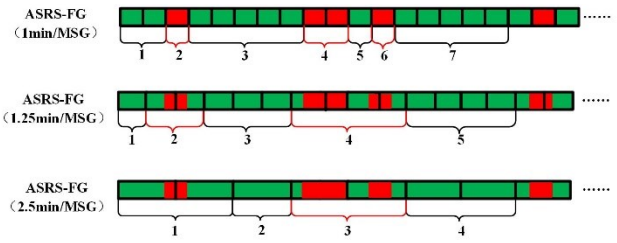

Fig. 6. Adaptive snapshot partition based on flexible granularity

Within each snapshot, we propose a shortest path algorithm to avoid the use of risky links. We can get the interruption start and end time and risk type of the link in Section II. Then we define that R represents the risk situation of the link, which is regarded as an important link weight influence factor., The value of R of high-risk links is infinite, that of low-risk links is constant A, and that of zero-risk links is 1. Specifically, we consider that the link weight is LW = αRD/B, then the total weight of the path is $\sum_1^i LW_i$, Where i is the number of links on the path, D is the link distance, B is the percentage of residual bandwidth, and α is the power loss. Finally, the shortest path algorithm is used for routing calculation, which effectively avoids the use of risky links and improves the service success ratio. The logic code of the ASRS-FG algorithm is as follows, the time complexity is O (n), and n is the number of MSGs.

Algorithm: Adaptive snapshot routing algorithm based on flexible granularity (ASRA-FG)

Input: L : length of minimum snapshot granularity (MSG); T : maximum length of a snapshot; i : serial number of MSG; S : risk link set; C : topology cycle; M : set of snapshots with no-risk MSGs which are not risky; N : set of snapshots with risky MSGs.

Output: service path P.

1. Divide a periodic network topology into C/L MSGs ;

2. Map the time period of S to the corresponding MSG, and mark these MSGs as risky;

3. For (i = 1; i <= C/L; i++)

    If k consecutive MSGs are not risky, and k <= T/L, then

        divide these k MSGs into a snapshot of M;

    If k consecutive MSGs are not risky, and k > T/L, then

        divide T/L MSGs into a snapshot of M;

        divide the remaining less than T/L MSGs into another snapshot of M;

    If MSG i is risky, and adjacent MSGs are not risky, then

        divide MSG i into a snapshot of N;

    If k consecutive MSGs are risky, and k <= T/L, then

        divide these k MSGs into a snapshot of N;

    If k consecutive MSGs are risky, and k > T/L, then

        divide T/L MSGs into a snapshot of N;

        divide the remaining less than T/L MSGs into other snapshot of N;

9. The high-risk link weight influence factor R=∞ in snapshots of N, the low-risk link R = A, A is the constant;

10. Use Depth First Search (DFS) to calculate all paths between source and sink nodes;

11. Calculate the weights of all paths and select the path with the smallest weight as the service path P;

12. Return service path P.

IV. SIMULATION SETTINGS AND RESULTS

A. Simulation Settings

In order to verify the performance of the adaptive snapshot routing strategy based on spatial risk perception, we built a single-layer Iridium-like network simulation platform composed of an ONOS-based SDN controller and Mininet nodes. Each satellite has four inter satellite links, two of which are intra orbit links and two are inter orbital links. There is no

link connection between tracks 1 and 6 due to the reverse gap, and the satellite optical networks topology is shown in Fig. 7. The specific track parameters are shown in Table IV.

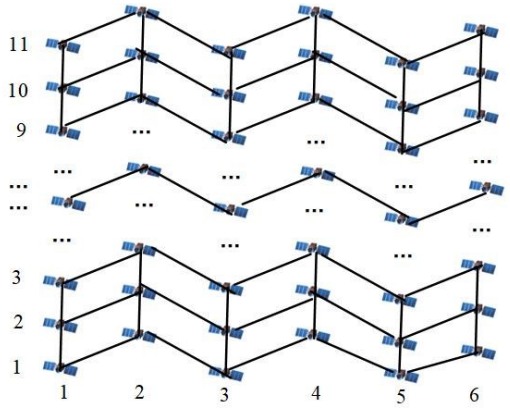

Fig. 7. Iridium-like network topology

TABLE IV. SATELLITE ORBIT PARAMETERS

Orbit Type	LEO
Orbital Height (km)	758
Orbital Inclination (°)	86
Number of Satellites	66
Number of Orbital Planes	6
Number of Satellites per Orbit	11
Phase Factor	0

B. *Simulation Results*

Since snapshot switching will cause short-term transmission interruption and routing instability, the fewer snapshot switching times, the better. However, if the snapshot duration is too long, each snapshot cannot effectively reflect network topology changes. Therefore, the selection of the appropriate minimum snapshot granularity and the division of snapshots have an important impact on the performance of satellite optical networks routing and transmission. In order to verify the performance of ASRS, we conducted simulations from three aspects: snapshot switching times, service success ratio and average link available time. In this simulation, for ASRS-FG, the snapshot duration T under risk-free conditions is 5 minutes, and the MSG duration t is 1, 1.25, and 2.5 minutes, respectively. For ESS, the snapshot duration is 1, 1.25, 2.5, and 5 minutes respectively.

First, as shown in Fig. 8, we compare snapshots switching times in a cycle between ASRS-FG and ESRS under different MSG conditions. The abscissa is the ratio of the time of space debris causing risk to the link in a cycle time, which is called the percentage of debris risk time (PDRT). For example, PDRT = 25% means that there are inter-satellite links affected by space debris in 25% of a topology cycle time. It can be seen that for ASRS-FG, under the same MSG, the number of snapshots increases with the increase of PDRT, and the smaller the BSG, the more snapshot switching. In addition, it can be clearly seen that in a cycle, under the same MSG condition, snapshots switching times of ASRS-FG is much smaller than that of ESRS. Compared to ESRS, snapshot switching times of ASRS-FG is reduced by an average of 54.88%, that is, fewer snapshots are stored on the satellite, which greatly saves the more storage space on the satellite, and reduces the on-board processing burden.

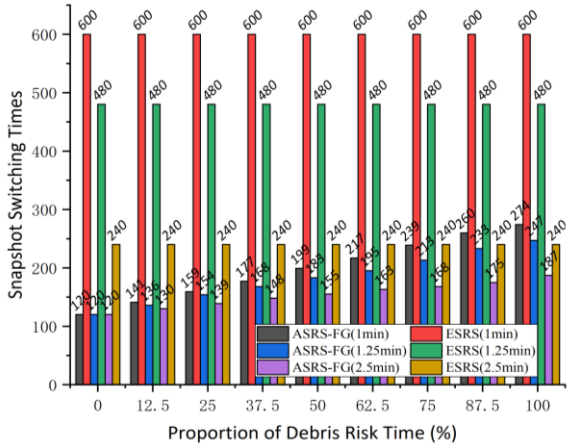

Fig. 8. Snapshot switching

Fig.9 shows that for different MSG, with the increase of the percentage of debris risk time (PDRT), the service success ratio all decreases, because the more risk is, the more unusable links will be, the lower the routing and transmission performance will be. In addition, under the same PDRT condition, the smaller the MSG is, the higher the service success ratio will be. Because the smaller the MSG, the less time the snapshot affected by risk takes is, and the better routing performance will be. When PDRT is 0, since the snapshots divided by ASRS and ESRS are the same, they have the same success rate. Under the same MSG and PDRT conditions, the service success rate of ASRS-FG is about 5% higher than the equal-length snapshot routing strategy (ESRS), because the ASRS-FG can effectively avoid the use of risky links, at the same time greatly reduce snapshot switching times, thus reducing the service failure caused by snapshot switching.

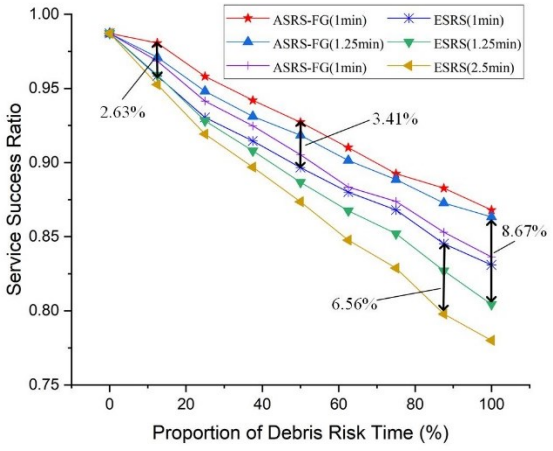

Fig. 9. Service success ratio

Finally, we define the proportion of average link available time (PALAT), which represents the ratio of average available time of all the links to the total length of a cycle. The higher the

PALAT is, the longer the link can be used in a cycle will be. As shown in Fig. 10, when the percentage of debris risk time is 0%, the proportion of average link available time is less than 100% because some links will be disconnected in the polar region for Iridium constellation. In the same MSG case, with the increase of the proportion of debris risk time, the PALAT decreases. This is because the number of links affected by debris is more. In addition, under the same proportion of debris risk time, the smaller the MSG is, the higher the average available time of the links will be. This is because the snapshot duration of the link affected by debris is shorter, and the link can be used for a longer time. Under the same MSG and PDRT, compared with ESRS, the PALAT of ASRS-FG is about 2% lower than ESRS, because longer snapshot duration causes the risky link to be unusable for longer.

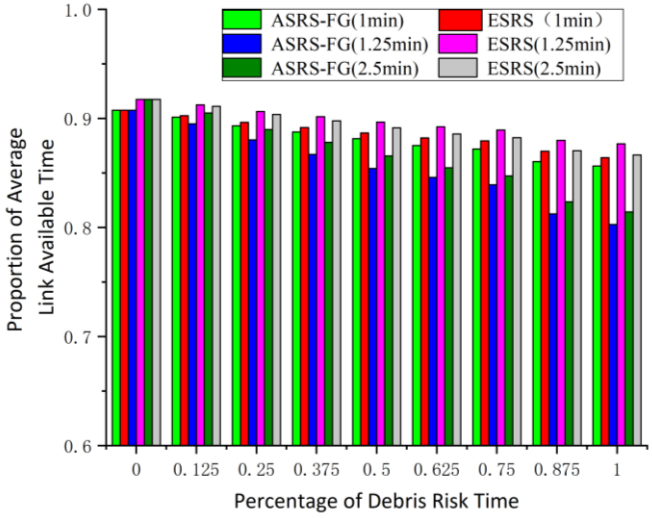

Fig. 10. Proportion of average link available time (PALAT)

V. CONCLUSIONS

In this paper, we construct a physical model of inter-satellite laser link interruption caused by space debris, and propose a space debris risk perception model based on machine learning. The results show that the accuracy of the model reaches 95%. In addition, we propose an adaptive snapshot routing strategy based on flexible granularity (ASRS-FG), which can effectively avoid the use of risky links. Finally, we built a satellite optical networks simulation platform based on ONOS. Compared with the equal-length snapshot routing strategy (ESRS), the service success rate of ASRS-FG increases by about 5%, and the snapshot switching times decrease by 54.88% on average.

ACKNOWLEDGMENT

This work has been supported in part by National Natural Science Foundation of China (NSFC) (61822105, 61010201).

REFERENCES

[1] Sun, Kui, Zhe Wang, Yuanfei Zhang, and Hong Liu. "Triaxial contact detumbling of large-scale space debris." In 2018 IEEE 3rd Advanced Information Technology, Electronic and Automation Control Conference (IAEAC), pp. 1840-1844. IEEE, 2018.

[2] Chengzhuo, Wang, Liu Suyang, Guo Xiye, and Yang Jun. "Dynamic optimization of laser inter-satellite link network topology based on genetic algorithm." In 2019 14th IEEE International Conference on Electronic Measurement & Instruments (ICEMI), pp. 1331-1342. IEEE, 2019.

[3] Arnon, Shlomi, and N. S. Kopeika. "Laser satellite communication network-vibration effect and possible solutions." Proceedings of the IEEE 85, no. 10 (1997): 1646-1661.

[4] Luo, Kenneth CK, R. Y. C. Chow, and R. Newman-Wolfe. "An efficient algorithm for reconfiguration of large-scale point-to-point satellite computer networks with maximum connectivity." In 1990 Ninth Annual International Phoenix Conference on Computers and Communications, pp. 194-195. IEEE Computer Society, 1990.

[5] Laghezza, F., F. A. B. R. I. Z. I. O. Berizzi, A. Capria, E. N. Z. O. Dalle Mese, G. Pupillo, S. Montebugnoli, E. Salerno, and M. Di Martino. "Italian bistatic radar system for surveillance of space debris in Low Earth Orbit." In 2010 IEEE Radar Conference, pp. 220-224. IEEE, 2010

[6] Ganguli, Gurudas. "Increasing hazards of orbital debris: Cause, effect, and mitigation." In 2015 1st URSI Atlantic Radio Science Conference (URSI AT-RASC), pp. 1-1. IEEE, 2015.

[7] Kessler, Donald J., and Burton G. Cour‐Palais. "Collision frequency of artificial satellites: The creation of a debris belt." Journal of Geophysical Research: Space Physics 83, no. A6 (1978): 2637-2646.

[8] Rafique, Danish, and Luis Velasco. "Machine learning for network automation: overview, architecture, and applications [Invited Tutorial]." Journal of Optical Communications and Networking 10, no. 10 (2018): D126-D143.

[9] Yang, Jianan, Yu Hen Hu, Yong Liu, Xiaolei Hou, and Quan Pan. "On the Application of Reinforcement Learning in Multi-debris Active Removal Mission Planning." In 2019 IEEE 28th International Symposium on Industrial Electronics (ISIE), pp. 605-610. IEEE, 2019.

[10] Peng, Hao, and Xiaoli Bai. "Improving orbit prediction accuracy through supervised machine learning." Advances in Space Research 61, no. 10 (2018): 2628-2646.

[11] Hassanien, Aboul Ella, Ashraf Darwish, and Sara Abdelghafar. "Machine learning in telemetry data mining of space mission: basics, challenging and future directions." Artificial Intelligence Review 53, no. 5 (2020): 3201-3230.

[12] Zhu, Yu, Lanlan Rui, Xuesong Qiu, and Haoqiu Huang. "Double-layer Satellite Communication Network Routing Algorithm Based on priority and failure probability." In 2019 15th International Wireless Communications & Mobile Computing Conference (IWCMC), pp. 1518-1523. IEEE, 2019.

[13] Tang, Zhu, Zhenqian Feng, Wei Han, Wanrong Yu, Baokang Zhao, and Chunqing Wu. "Improving the snapshot routing performance through reassigning the inter-satellite links." In 2015 IEEE Conference on Computer Communications Workshops (INFOCOM WKSHPS), pp. 97-98. IEEE, 2015.

[14] Tan, Haichao, and Lidong Zhu. "A novel routing algorithm based on virtual topology snapshot in LEO satellite networks." In 2014 IEEE 17th International Conference on Computational Science and Engineering, pp. 357-361. IEEE, 2014.